Int. J.Nano Dimens. 6(1): 55-66, Winter 2015
ISSN: 2008-8868

Contents list available at **IJND**

International Journal of Nano Dimension

Journal homepage: *www.IJND.ir*

Adsorption kinetics and thermodynamics of Malachite Green from aqueous solutions onto expanded Graphite nanosheets

Gh. Kiani *

School of Engineering-Emerging Technologies, University of Tabriz, Tabriz, Iran.

Received 02 July 2013
Accepted 22 October 2013

* Corresponding author:
Gholamreza Kiani
School of Engineering-Emerging Technologies, University of Tabriz, Tabriz, Iran.
Tel +98 4113393853
Fax +98 4113294626
Email g.kiani@tabrizu.ac.ir

ABSTRACT

Expanded graphite nanosheets (EG-nanosheets) were used for adsorption of Malachite Green (MG) from aqueous solution. The influences of dye concentrations, absorbent dosage, pH values and the temperatures on the adsorption were investigated as well. The dye adsorption experiments were carried out by utilizing batch procedure. EG-nanosheets were initially characterized by scanning electron microscopy (SEM), fourier transform infrared (FT-IR) and X-ray diffraction (XRD). Adsorption efficiency increased with increment in initial pH, dye concentration and temperature, but decreased with increment in adsorbent dose. The rate parameters of adsorption were evaluated by First-order, pseudo-second-order, and intraparticle diffusion models. These data indicated an endothermic spontaneous adsorption process and kinetically followed the pseudo-second order model with activation energy of +17.44 $kJmol^{-1}$. Langmuir, Freundlich and Temkin equations were used for analyzing of experimental isotherm data and found that the Langmuir isotherm model showed good fit to the equilibrium adsorption data. The maximum adsorption capacity of 158.9 $mg\ g^{-1}$ of Malachite Green was achieved (dye initial concentration of 100 $mg\ L^{-1}$). Thermodynamic parameters such as changes in the free energy of adsorption ($\Delta G°$), enthalpy ($\Delta H°$) and entropy ($\Delta S°$) were calculated. The negative values of $\Delta G°$ indicate that the malachite green adsorption process is spontaneous in nature and the positive value of $\Delta H°$ shows the endothermic nature of the process. Adsorption onto EG has proved to be highly efficient technique for the handling of dye-contaminated waters.

Keywords: *Expanded Graphite Nanosheets; Nano-adsorbent; Textile dye; Kinetic model; Thermodynamic parameter.*

INTRODUCTION

Carbonic materials like activated carbon which have adsorptive particles or granules usually obtained by heating carbonaceous material in the absence of air or in steam and possessing a high capacity to selectively remove trace and soluble components such as organic dyes from solution [1, 2].

Expanded graphite (EG) is from graphite intercalation compounds (expandable graphite), and it possesses abundant porous structure and high surface area and structure with the size from several nm to hundreds μm. Expanded graphite was used as an absorbent with a high adsorption capacity for dyes and heavy metal ions [3-4].

Malachite green dye is commonly used for the dyeing process and in the manufacturing of paints and printing inks [5]. Also upon contact with eye will lead to permanent injury of human eyes and laboratory animals. Therefore effective removal of malachite green from wastewater is necessary. Techniques evaluated for MG removal include photo-degradation [6], photo-catalytic degradation [7], bioremediation [8], and adsorption [9]. Adsorption has gained importance as an effective purification and separation technique used in water and wastewater treatment. The removal of metals, colored and colorless organic pollutants from industrial wastewater are considered an important application of adsorption processes using suitable adsorbents. A considerable amount of work has also been reported in the literatures regarding the adsorption of some dyes on various adsorbent surfaces such as activated carbon [1,2], silica [10], clay [9], natural polymers [11] and so forth.

The aim of this study is investigating the adsorption capacity of EG-nanosheets for MG removal from aqueous solution. Thus, the present study is devoted to test the ability of EG-nanosheets for removing MG. Several studies have been proposed in the literature about the use of new sorbents, in relation with MG sorption from water solutions. These materials have some comparative advantages in contrast to common sorbent materials. Some remarkable studies can be seen in Table 1. The recovery percentage of MG onto EG nanosheets is much more than other absorbents [12-21]. Effective parameters such as adsorbent dosage, initial dye concentration, pH, temperature, kinetics, and thermodynamic studies were investigated.

Table 1. Comparison of Adsorption Capacities of Various Adsorbents for Malachite Green.

Absorbents	q_t (mg/g)	Reference
Rattan Sawdust	62.71	16
Ferrofluid Mdified Sawdust	43	17
Magnetically Labeled Baker's Yeast Cells	19.6	18
Hydrilla verticillata	91.97	19
Solid Agricultural Waste	39.84	20
Wheat bran coarse particle	75.64	21
Mango seed husk	47.9	22
Rice husk activated carbon	63.85	23
PETNa8	169.49	24
MCM-48	158.7	25
Expanded graphite nanosheets	158. 9	Present Work

EXPERIMENTAL

Materials

A SEM image was obtained with a FE-SEM Hitachi S-4700 and Fourier Transform Infrared (FT-IR) spectroscopy was performed on ABB, MB3000 spectrometer. X-ray diffraction (XRD) study was carried out with D500 Siemens, X-Ray diffractometer. Analytical reagent grade Malachite Green (MG, $C_{23}H_{25}N_2Cl$) was purchased from Merck Co. It has a maximum visible absorbance at a wavelength of 621 nm. MG stock solution was prepared by dissolving an accurately weighed amount of MG in distilled water to achieve a concentration of 500 mg L^{-1} and subsequently diluted to the required concentrations.

Adsorption procedure

Batch adsorption experiments were conducted in order to evaluate the effects of contact time, solution pH, adsorbent dose, initial MG concentration and temperature. Batch adsorption

experiments were carried out typically described in literature [9].

The amount of MB adsorbed by EG nanosheets in each time interval *t*, q_t, was calculated by equation (1):

$$q_t = V(C_0 - C_t)/W \quad (1)$$

Where q_t is the amount of adsorbed dye on EG-nanosheets at any time (mg g^{-1}); C_0 and C_t are concentration of MG before adsorption and after contact time *t* (mg L^{-1}), respectively; *V* is the volume of MG solution (L), and *W* is the mass of EG-nanosheets sample used (g) [22].

The kinetics of the adsorption process was analyzed using the pseudo first-order, pseudo second-order and intraparticle diffusion equations to model the kinetics of MG adsorption onto EG nanosheets. The linear forms of three models are expressed by equation (2-4):

$$\ln(q_e - q_t) = \ln q_e - k_1 t \quad (2)$$

$$\frac{t}{q_t} = \frac{1}{k_2 q_e^{\,2}} + \frac{1}{q_e} t \quad (3)$$

$$q_t = k_i t^{1/2} + C \quad (4)$$

Where q_e is the amount of the adsorbed pollutant at equilibrium per unit mass of the adsorbent (mg g^{-1}), k_1 (min^{-1}), k_2 (g mg^{-1} min^{-1}) and k_i (mg g^{-1} $min^{-1/2}$) are the rate constants of the pollutant adsorption in pseudo-first-order (Eq. 2), pseudo-second-order (Eq. 3) and intraparticle diffusion models (Eq. 4), respectively [23-25].

RESULTS AND DISCUSSION

Characterization of Expanded graphite nanosheets

SEM images of natural Graphite (Figure 1a) and expanded graphite flakes (Figure 1b and c) are shown in Figure 1. Furthermore, Figure 1(b and c) shows that the individual graphite nanosheets is not a single graphite nanosheets or ‘‘graphene’’ but rather consists of several layers of graphite sheets. It is important to know that the graphite nanosheets contain functional groups for instance hydroxyl and carboxylic acid after acid and high temperature treatments [26, 27]. Functional groups of EG-nanosheets provide Physical interaction with organic dyes. Acid and high temperature treatments endows EG with high surface area, corresponding to graphite nanosheets having thickness between 50–100 nm.

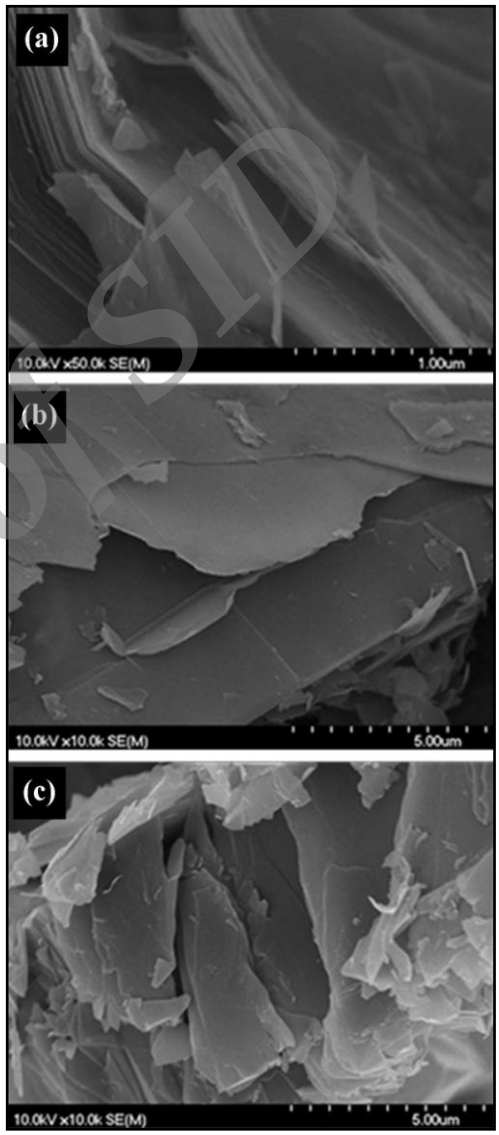

Fig. 1. SEM micrographs of a) Natural graphite and b,c) expanded graphite nanosheets.

Figure 2a shows FT-IR spectrum of graphite. The results show that the graphite exhibits no functional groups on the surface. The peak at 1560 cm^{-1} is of the C–C–C symmetric

stretching vibration. The broad absorption band at 3400 cm^{-1} indicates O–H stretching vibration, whereas the band at 2924 cm^{-1} is due to the stretching of the C–H bonds. In FT-IR spectra of EG (Figure 2b), some new peaks are observed at lower wave number in between 500–800 cm^{-1} due to the C–H outer bending vibration, C–H in plane bending and out-of-plane C–H wagging [28, 29]. The peak at 3436 cm^{-1} is attributed to the O–H stretching vibration of phenolic or alcoholic functional groups present on the EG surface. The band at 1706 cm^{-1} can be ascribed to the C=O stretching of COOH groups, The strong band at 1050 cm^{-1} is due to the vibration of C-O, and the weak band at 1200 cm^{-1} will be due to phenolic groups. During intercalation of natural graphite by strong acids some of the carbon double bonds are oxidized, which leads to the formation of oxygen-containing functional (carboxylic and hydroxyl) groups on exfoliated graphite surface, that can facilitate the physical and chemical interactions with dyes [30].

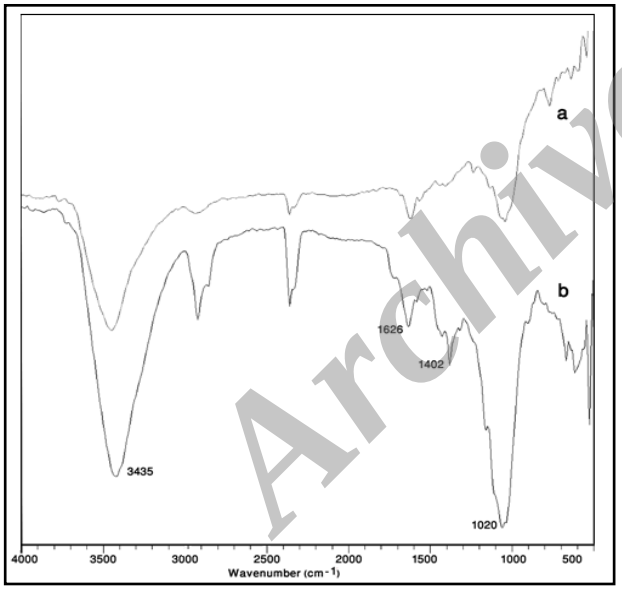

Fig. 2. FT-IR spectra of a) graphite and b) EG-nanosheets.

XRD analysis of graphite and EG nanosheets were studied (Figure not shown here). XRD analysis indicates a very intense and narrow peak at 26.62, 44.60, and 54.85°. These peaks match with the (002), (101), and (004) planes of the hexagonal system (reference number PCPDFWIN 25-0284) of the EG [31].

Adsorption rate

- ***Effect of contact time and initial dye concentration***

The experimental results of adsorption of MG onto EG-nanosheets at the various initial concentrations of 20, 60 and 100 mg L^{-1} is illustrated in Figure 3. Figure 3 reveals that adsorption capacity of the adsorbent increased from 0.093 to 0.431 mmol g^{-1} (35.2 to 158.9 mg g^{-1}) with increase in dye concentration. This indicates that the initial dye concentration plays an important role in the adsorption capacity of malachite green onto EG-nanosheets. At lower concentration, the ratio of initial number of dye molecules to the available surface area is low. Subsequently, the fractional adsorption becomes independent of initial dye concentration.

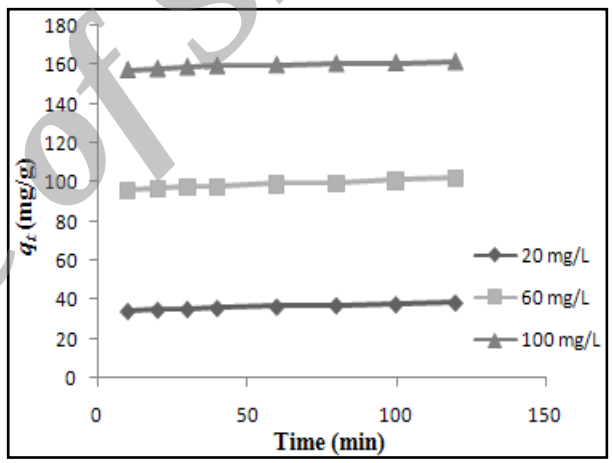

Fig. 3. Effect of contact time and initial dye concentration on adsorption of MG onto EG-nanosheets from aqueous solutions (T=30 °C, pH=8.5).

- ***Effect of pH***

One of the most important factors affecting the adsorption capacity is pH. The adsorption of MG increases with decrease in the pH of the solution. It is well known that the surface of graphite contain some oxygen groups such as carboxylic groups (COOH) and hydroxylic groups (OH) after acid treatment [32]. When pH increases, the carboxylic groups are ionized and the negative charge density on the surface increases, resulting in enhanced removal efficiency of dyes. As can be cleared in Figure 4 (a and b), when pH of the dye solutions was increased from 7.5 to 8.5, the

amounts of dye adsorbed increased from 18.5 (46.4% removal) to 34.8 (87% removal) mg g^{-1}, respectively. The surface of the EG-nanosheets may contain a large number of negative active sites and therefore cationic MG dye can be related to these negative sites.

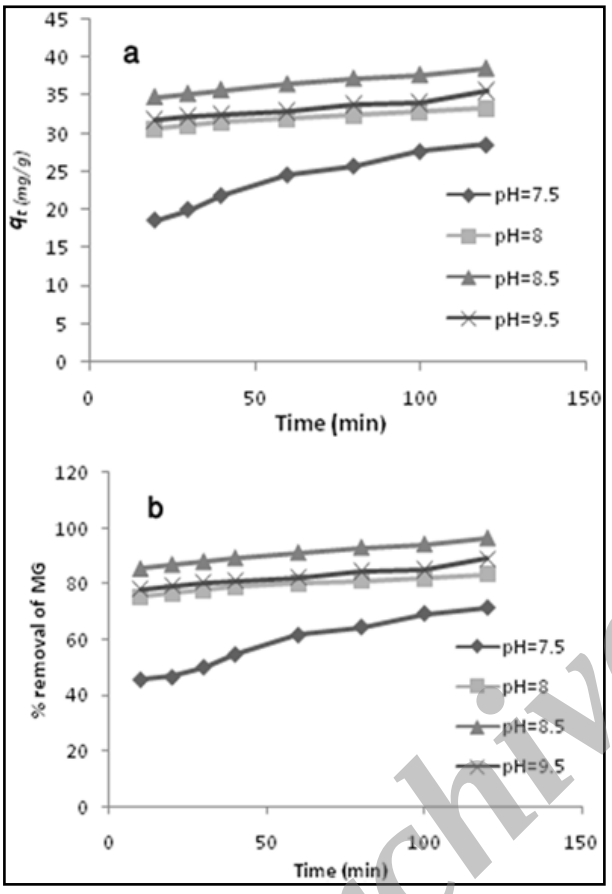

Fig. 4. Effect of contact time and initial pH on a) adsorption and b) % removal of MG onto EG-nanosheets from aqueous solutions (T=30 °C, $[MG]_0$=20mg L^{-1}, EG-nanosheets=0.05 g).

- ***Effect of adsorbent dose***

The effect of the adsorbent dose on removal of MG is depicted in Figure 5a. The effect of EG-nanosheets doses on MG adsorption was studied by varying the adsorbent dose from 0.05 to 0.15 g. Adsorption capacity decreases from 25.4 to 7.9 mg g^{-1} as the adsorbent dose increases from 0.05 to 0.15 g. This may be attributed to the aggregation of adsorbent particles at high dosage, which reduces the total surface area of the adsorbent and results in an increase in the diffusion path length [33].

- ***Effect of temperature***

In order to observe the effect of temperature batch adsorption studies were carried out with MG. Adsorption of MG onto EG-nanosheets was measured at three different temperatures (30, 45, and 60 °C). Figure 5b shows an increase in adsorption with an increase in solution temperature. Therefore, adsorption was endothermic in nature. The equilibrium adsorption capacity was clearly affected by temperature, with the amount of MG adsorbed increasing from 35.2 (88.1% removal) to 39.6 mg g^{-1} (99.1% removal) when the temperature was raised from 30 to 60ºC. This may be a result of increase in the mobility of the large dye ion with temperature. An increasing number of molecules may also acquire sufficient energy to undergo an interaction with active sites at the surface. Furthermore, increasing temperature may produce a swelling effect within the internal structure of the EG-nanosheets enabling large dyes to penetrate further [33-34].

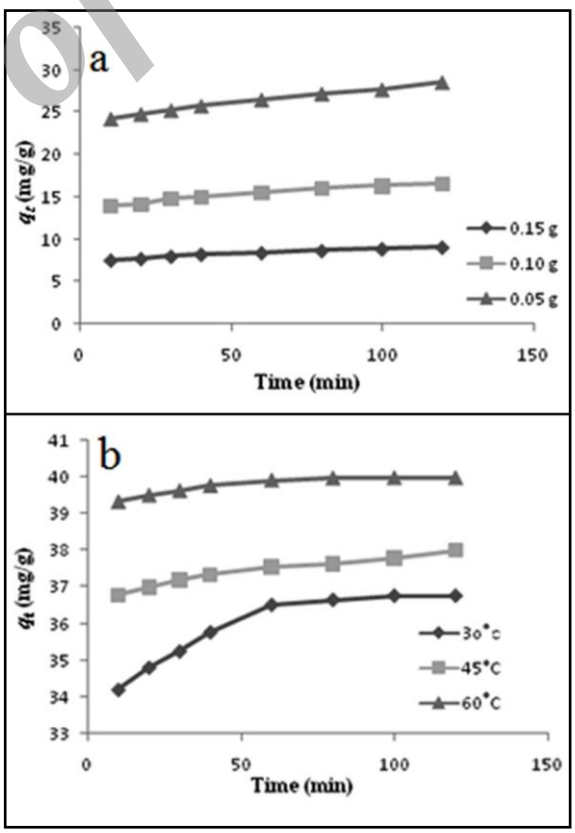

Fig. 5. Effect of adsorbent dose on adsorption of MG onto EG-nanosheets (T=30 °C, $[MG]_0$=20 mg L^{-1}, pH=8.5) and b) Effect of contact time and temperature on the removal rate of MG onto EG-nanosheets from aqueous solutions ($[MG]_0$=20mg L^{-1}, pH=8.5, EG-nanosheets=0.05 g).

Kinetics of adsorption

In order to find out the potential rate-controlling steps involved in the process of adsorption, kinetic models were established. Three kinetic models, pseudo-first-order, pseudo-second-order and intra-particle diffusion, are adopted to investigate the adsorption process at different temperatures [35]. Table 2 presented the rate constant and correlation coefficient of the pseudo-first-order, pseudo-second-order and the intraparticle diffusion model at 20, 40 and 60°C. The correlation coefficient R^2 for the pseudo-second-order adsorption model has extremely high values (R^2 > 0.999), and its calculated equilibrium adsorption capacities q_{ecal} fit well with the experimental data (Figure 6a). These suggest that the pseudo-second-order adsorption mechanism is predominant and the overall rate of this sorption process appears to be controlled by the chemical process [36].

Table 2. Adsorption kinetic parameters of MG onto Expanded graphite nanosheets

Temperature (˚C)	20	40	60
Pseudo-first-order			
K_1, min^{-1}	0.003	0.001	0.001
R^2	0.983	0.955	0.986
Pseudo-second-order			
K_2, g/mg min	199.9	44.3	10.9
$q_{e,\,cal}$ (mg g^{-1})	38	40.2	41.6
$q_{e,Exp}$ (mg g^{-1})	36.7	39.6	40.8
R^2	0.999	1	1
Intraparticle diffusion			
k_i, mg g^{-1} min$^{1/2}$	0.551	0.146	0.085
C	32.31	36.36	39.15
R^2	0.993	0.989	0.909

Adsorption isotherms

The analysis and design of sorption process requires the relevant Adsorption equilibria, which is the most important piece of information in the understanding an adsorption process. Adsorption isotherm is expressed by relating the amount of adsorbate taken up per gram of adsorbent, q_e (mg g^{-1}), to the equilibrium solution concentration, C_e (mg L^{-1}), at a fixed temperature [36].

In this study, three isotherms Langmuir (Eq. (5)) [37], Freundlich (Eq. (6)) [38] and Temkin (Eq. (7)) [39] were tested.

$$\frac{C_e}{q_e} = \frac{1}{K_L} + \frac{a_L}{K_L} C_e \qquad (5)$$

$$\log q_e = \log K_F + \frac{1}{n} \log C_e \qquad (6)$$

$$q_e = B_1 \ln K_T + B_1 \ln C_e \qquad (7)$$

Here q_e is the solid phase equilibrium concentration, i.e., the amount of MG adsorbed per unit weight of the EG-nanosheets (mg g^{-1}); C_e is the liquid phase equilibrium concentration (mg L^{-1}), K_L and a_L are Langmuir constants found from the intercept and slope of the straight line of the plot C_e/q_e versus C_e. The a_L constant is related to the free energy or net enthalpy of adsorption (L mg^{-1}) (a_L α $e^{-\Delta H/RT}$) [40], and K_L is the equilibrium constant of Langmuir (L g^{-1}). K_F is a Freundlich constant indicative of the relative adsorption capacity of the adsorbent (mg g^{-1}) and 1/n is the adsorption intensity. B_1 = RT/b, K_T is the equilibrium binding constant (Lmg^{-1}) and B_1 is the heat of adsorption.

Table 3 summarizes the values of k_L and a_L (Langmuir isotherm), K_F and 1/n (Freundlich isotherm), B_1 and k_T (Temkin isotherm) and the correlation coefficients for the three isotherms. It can be clear that the Langmuir model resulted into a better fit than the Freundlich and Temkin models. Langmuir isotherm model assumes uniform energies of adsorption on the surface without transmigration of adsorbate in the plane of the surface [36]. Therefore, the Langmuir isotherm model was chosen for estimation of the maximum adsorption capacity corresponding to complete monolayer coverage on the adsorbent surface. Similar result on the suitability of Langmuir isotherm was observed by the adsorption of methylene blue onto activated carbon [41]. Figure 6b shows Langmuir isotherms in the various temperatures.

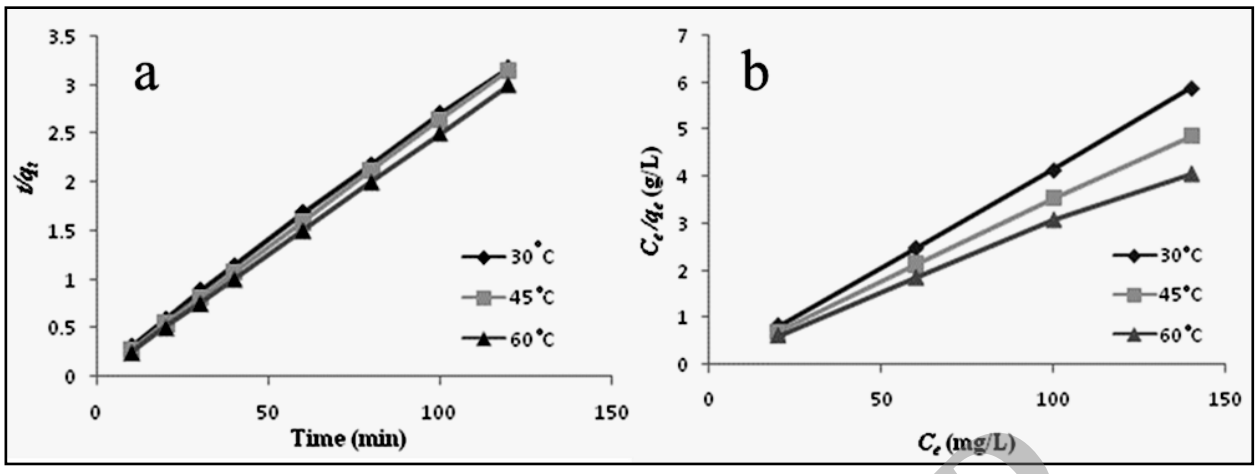

Fig.6. Pseudo-second-order plots for the adsorption of MG onto EG-nanosheets at various temperatures ($[MG]_0$=20mg L^{-1}, EG-nanosheets=0.05 g, pH=8.5) and b) Langmuir plot of adsorption of MG onto EG-nanosheets at various temperatures (pH=8.5, EG-nanosheets=0.05 g, $[MG]_0$= 20, 60, 100 and 140 mg L^{-1}).

Table 3. Langmuir, Freundlich and Temkin isotherm constants for MG adsorption onto EG-nanosheets

	Langmuir					***Freundlich***				***Temkin***			
Temperature (°C)	K_L	a_L	R_L	R^2	S	$1/n$	K_F	R^2	S	B_1	K_T	R^2	S
30	111.1	0.45	0.042	1	0.0056	0.018	32.37	0.977	0.023	28.17	10.71	0.993	0.125
45	136	0.95	0.020	0.999	0.0076	0.0055	38.61	0.962	0.045	-	-	-	-
60	200	1	0.019	1	0.0145	0.007	35.95	0.993	0.065	-	-	-	-

The essential characteristics of the Langmuir isotherm can be expressed by a dimensionless constant called the separation factor, R_L, [42] which is defined by

$$R_L = \frac{1}{1 + a_L C_o} \qquad (8)$$

The value of R_L indicates the type of the isotherm to be (i) unfavorable (R_L > 1), (ii) linear (R_L = 1), (iii) favorable (0 < R_L < 1), or (iv) irreversible (R_L = 0). The R_L values for the adsorption of MG onto EG-nanosheets are in the range of 0.019-0.042, indicating that the adsorption is a favorable process.

The standard deviation is a measure of how precise the average is, that is, how well the individual numbers agree with each other. It is a measure of a type of error called random error- the kind of error people can't control very well. It is calculated as follows:

$$S = \sqrt{\frac{\sum (Xi - \overline{X})^2}{n-1}} \qquad (9)$$

Here $\overline{X}$ is the average result and n is summing the individual results. The calculated amount of standard deviation of relative errors for three models was shown in Table 3. Based on data in Table 3, Langmuir is the best-fitting isotherms which had the highest coefficient of determination compared with other methods.

Adsorption thermodynamics

When the temperature is concerned for sorption, it is useful to determine the thermodynamic parameters such as standard Gibbs free energy change ΔG°, standard enthalpy change ΔH°, and standard entropy change ΔS°. The Gibbs free energy change for sorption of MG on EG-nanosheets is estimated by using equilibrium constant K_L [43]. The thermodynamic parameters ΔH^o, ΔS^o, and ΔG^o associated with the adsorption process can be determined by using the equations (10 and11).

$$\Delta G° = -RT ln K_L \qquad (10)$$

$$\Delta G° = \Delta H° - T\Delta S° \qquad (11)$$

Where K_L is Langmuir constant when concentration terms are expressed in L mol^{-1}, R (8.314 J mol^{-1} K^{-1}) is the universal gas constant and T (K) is the temperature. The spontaneous nature of sorption appears due to negative values of ΔG°. Figure 7a shows just such a plot with a correlation coefficient of 0.985. ΔH^o and ΔS^o values are thus found to be +241.1 kJmol^{-1} and +116.1 J K^{-1}, respectively, while the ΔG^o values are -11.8, -12.7, and -14.6 kJmol^{-1} (at 30, 45, and 60°C, respectively). This confirms affinity of EG-nanosheets for the MG. The positive ΔH° values could lead to endothermic nature of interaction between MG dye and EG-nanosheets adsorbent. Standard entropy determines the disorderness of the adsorption at solid–liquid interface [44].

Activation parameters

As shown earlier, the pseudo-second-order model is identified as the best kinetic model for the adsorption of MG onto EG-nanosheets. Accordingly, the rate constant k_2 of the pseudo-second-order model is adopted to calculate the activation energy (E_a) of the adsorption process using the Arrhenius equation (Eq. (12)), it is possible to gain some insight into the type of adsorption.

$$ln k_{sm} = ln A - E_a/RT \qquad (12)$$

Here E_a is the activation energy (J mol^{-1}), k_{sm} the pseudo-second-order rate constant for adsorption (g mol^{-1} s^{-1}), A the temperature-independent Arrhenius factor (g mol^{-1} s^{-1}), R the gas constant (8.314 J K^{-1} mol^{-1}), and T the solution temperature (K). The activation energy can be determined from the slope of the plot of $ln\ k_2$ versus 1/T. The physisorption process usually has the activation energy (Ea) in the range of 5-40 kJ mol^{-1}, while the activation energy (E_a) in the range of 40–800 kJ mol^{-1} suggests the chemisorption process [45]. The present results give E_a = +17.44 kJ mol^{-1} for the adsorption of MG onto EG-nanosheets (Figure 7b), confirming that the adsorption process of physisorption was predominant. The value is consistent with those found in the literature for the adsorption of dyes onto many adsorbents, e.g., MG onto HNTs (18.28 kJ mol^{-1}) [9] and methylene blue onto perlite (14 kJ mol^{-1}) [45].

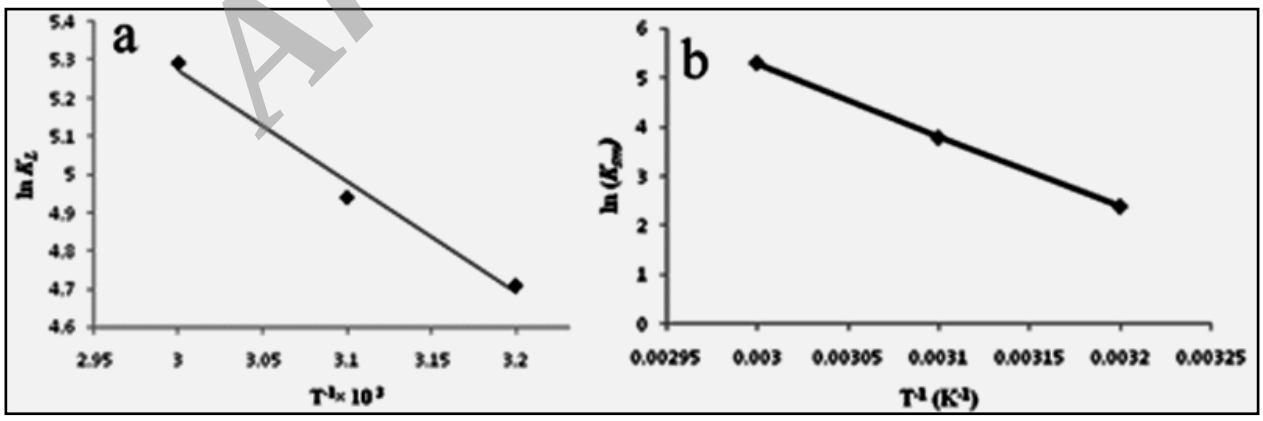

Fig. 7. Plot of lnK_L vs. T^{-1}: estimation of thermodynamic parameters for the adsorption of MG onto EG-nanosheets and b) Plot of lnk_{sm} vs. T^{-1}: estimation of the activation energy, E_a, for the adsorption of MG onto EG-nanosheets.

In this work, the MG was adsorbed on EG-nanosheets aggregated together to millimeter scale particles and were deposited completely within 30 min (Figure 8). This is also an advantage of the application of EG-nanosheets as a relative low-cost unconventional nano-adsorbent of MG.

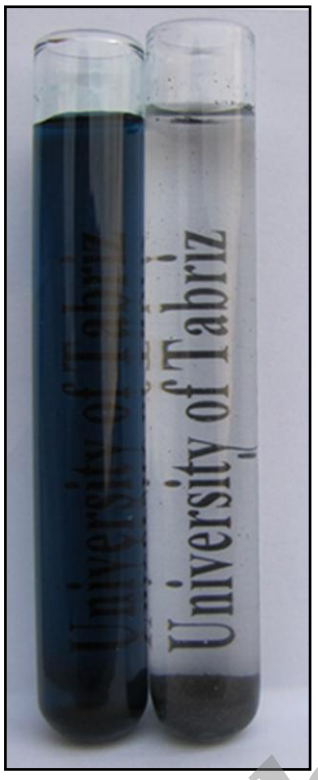

Fig. 8. The photos of the MG solution before (left) and after (right) adsorption with EG-nanosheets.

CONCLUSIONS

This work has demonstrated that EG-nanosheets can be employed as effective nano-absorbent for MG removal. The equilibrium data have been analyzed using Langmuir, Freundlich and Temkin isotherms. The characteristic parameters for each isotherm and pertinent correlation coefficients have been determined. Langmuir model fitted well and adsorption was of second-order kinetics. A maximum adsorption capacity of 158.9 mg g^{-1} of Malachite Green was achieved. The adsorbed amount of MG increased as initial MG concentration, pH and temperature increase. The adsorption of MG onto EG-nanosheets obeyed pseudo-second-order kinetics with activation energy +17.44 kJ mol^{-1}, this is consistent with the description of the process as physisorption. The negative values of $\Delta G°$ and positive value of $\Delta H°$ show that the adsorption is a spontaneous and endothermic process. The dimensionless separation factors (R_L) released that the adsorption is a favorable process. It is expected that the EG-nanosheets can be utilized as unconventional nano-adsorbent for the removal of dyes from aqueous solutions.

ACKNOWLEDGEMENTS

The authors wish to thank University of Tabriz for all the supports provided. We would like to thank Mr. Ali Haddadpour for his kind cooperation.

REFERENCES

[1] Yasin Y., Hussein M. Z, Ahmad F. H., (2007), Adsorption of methylene blue onto treatedactivated carbon. *Malays. J. Anal Sci.* 11: 400-406.

[2] Calvete T., Lima E. C., Cardoso, N. F., Dias S. L. P., Ribeiro E. S., (2010), Removal of Brilliant Green Dye from Aqueous Solutions Using Home Made Activated Carbons. *Clean-Soil Air Water*. 38: 521-532.

[3] Zhang J., Li Y., Zhang C., Jing C. Y., (2008), Adsorption of malachite green from aqueous solution onto carbon prepared from Arundo donax root. *J. Hazard. Mater*. 150: 774-782.

[4] Bansal R. C., Goyal M., (2005), Activated Carbon Adsorption, *CRC Press.Boca Raton, FL*.

[5] AltInIsIk A., Gür E., Seki Y., (2010), A natural sorbent, Luffa cylindrica for the removal of a model basic dye. *J. Hazard. Mater*. 179: 658-664.

[6] Zhou X., Lan J., Liu G., Deng K., Yang Y., Nie G., Yu J., Zhi L., (2012), Facet-Mediated Photodegradation of Organic Dye

over Hematite Architectures by Visible Light. *Angew. Chem. Internat. Ed*. 51: 178-182.

[7] Khataee A. R., Zarei M., Pourhassan M., (2010), Bioremediation of Malachite Green from Contaminated Water by Three Microalgae: Neural Network Modeling, *Clean- Soil Air Water*. 38: 96-103.

[8] Umrania V. V., (2006), Bioremediation of toxic heavy metals using acidothermophilic autotrophies. *Biores. Technol*. 97: 1237-1242.

[9] Kiani G. R., Dostali M., Rostami A., Khataee A.R., (2011), Adsorption studies on the removal of Malachite Green from aqueous solutions onto halloysite nanotubes. *Appl. Clay Sci*. 54: 34-39.

[10] Najafi M., Yousefi Y., Rafati A. A., (2012), Synthesis, characterization and adsorption studies of several heavy metal ions on amino-functionalized silica nano hollow sphere and silica gel. *Separ. Purif. Tech*. 85: 193–205.

[11] Abdel-Halim E. S., Al-Deyab S. S., (2011), Removal of heavy metals from their aqueous solutions through adsorption ontonatural polymers. *Carbohyd. Polym*. 84: 454-458.

[12] Hameed B. H., El-Khaiary M. I. (2008), Malachite green adsorption by rattan sawdust: Isotherm, kinetic and mechanism modeling. *J. Hazard. Mater*. 159: 574-579.

[13] Safarik I., Lunackova P., Mosiniewicz-Szablewska E., Weyda F., Safarikova M., (2007), Adsorption of water-soluble organic dyes on ferrofluidmodified Sawdust, Holzforschung. 61: 247-253.

[14] Safarik I., Ptackova L., Safarikova M., (2002), Adsorption of dyes on magnetically labeled baker'syeast cells. *Eur. Cells Mater*. 3: 52-55.

[15] Rajeshkannan R., Rajasimman M., Rajamohan N., (2010), Removal of malachite green from aqueous solution using Hydrilla verticillata-optimization, equilibrium and kinetic studies. *Int. J. Civil Environ. Eng*. 2: 222-229.

[16] Shabudeen Syed P. S., (2011), Study of the Removal of Malachite Green from Aqueous Solution by using Solid Agricultural Waste. *Res. J. Chem. Sci*. 1: 1-117.

[17] Wang X. S., Zhou Y., Jiang Y., Sun C, (2008), The removal of basic dyes from aqueous solutions using agricultural by-products. *J. Hazard. Mater*. 157: 374-385.

[18] Franca A. S., Oliveira L. S., Saldanha S. A., Santos P. I. A., Salum S. S., (2010), Malachite green adsorption by mango (Mangifera indica L.) seed husks: Kinetic, equilibrium and thermodynamic studies. *Des. Water Treat*. 19: 241-248.

[19] Sharma Y. C., Singh Uma B., (2009), Fast Removal of Malachite Green by Adsorption on Rice Husk Activated Carbon. *Open Environ. Pol .Toxicol. J*. 1: 74-78.

[20] Akmil-Basar C, Onal Y., Kilicer T., Eren, D., (2005), Adsorption of high concentration malachite green by two activated carbon having different porous structures. *J. Hazard. Mater. B*. 127: 73-80.

[21] Anbia M., Ghaffari A., (2011), Removal of Malachite Green from Dye Wastewater Using Mesoporous Carbon Adsorbent. *J. Iran Chem. Soc*. 8: 67-76.

[22] Lalhruaitluanga H., Jayaram K., Prasad M. N. V., Kumar K. K., (2010), Lead (II) adsorption from aqueous solutions by raw and activated charcoals of Melocanna baccifera Roxburgh (bamboo) A comparative study. *J. Hazard. Mater*. 175: 311-318.

[23] Santhi T., Manonmani S., Smitha T., (2010), Kinetics and Isotherm Studies on cationic dyes adsorption onto *Annona Squmosa* Seed activated Carbon. *Int. J. Eng. Sci. Technol*. 2: 287-295.

[24] Bhatnagar A., Jain A. K., (2005), A comparative absorption study with different industrial wastes as adsorbents for removal of cationic dyes from water. *J. Colloid. Interf. Sci*. 281: 49-55.

[25] Alzaydien A. S., (2009), Adsorption of Methylene Blue from Aqueous Solution onto a Low-Cost Natural Jordanian Tripoli. *Am. J. Environ. Sci*. 5: 197-208.

[26] Chen G., Weng W., Wu D., Wu C., Lu J., Wang P., (2004), Preparation and characterization of graphite nanosheets from ultrasonic powdering technique. *Carbon*. 42: 753-759.

[27] Zheng W., Wong S. C., Sue H. J., (2002), Transport behavior of PMMA/expanded graphite nanocomposites. *Polymer*. 73: 6767- 6773.

[28] Si Y., Samulski E. T., (2008), Synthesis of water soluble grapheme, *Nano Lett*. 8: 1679-1682.

[29] Wu X., Qi S., He J., Duan G., (2010), High conductivity and low percolation threshold in polyaniline/graphite nanosheets composites. *J. Mater. Sci*. 45: 483- 489.

[30] Dhakate S. R., Sharma S., Borah M., Mathur R. B., Dhami T. L., (2008), Expanded graphite-based electrically conductive composites as bipolar plate for PEM fuel cell. *Int. J. Hydrogen Energy*. 33: 7146-7152.

[31] Konwer S., Gogoi J. P., Kalita A., Dolui S. K., (2011), Syn- thesis of Expanded Graphite Filled Polyaniline Compos- ites and Evaluation of Their Electrical and Electrochemi- cal Properties. *J. Mater .Sci. Mater. Electron*. 22: 1154-1161.

[32] Liu J., Rinzler A. G., Dai H. J., Hafner J. H., Bradley R. K., Boul P. J., Lu A., (1998), Fullerene pipes. *Science* 280: 1253-1256.

[33] Shukla A., Zhang Y. H., Dubey P., Margrave J. L., Shukla S. S., (2002), The role of sawdust in the removal of unwanted materials from water. *J. Hazard. Mater*. 95: 137-152.

[34] Tabrez K.A., Imran A., Vati S.V., Sangeeta S., (2009), Utilization of fly ash as low cost adsorbent for the removal of Methylene blue , Malachite green and Rhodamine-B dyes from Textile waste water. *J. Envion. Prot. Sci*. 3: 11-22.

[35] Santhi T., Manonman S., (2011), Malachite Green Removal from Aqueous Solution by the Peel of Cucumis sativa Fruit. *Clean – Soil Air Water*. 39: 162-170.

[36] Papinulti L., Mouso N., Forchiassin F., (2006), Removal and degradation of the fungicide dye malachite green from aqueous solution using the system wheat bran – Fomessclerodermeus. *Enzy. Microb. Technol*. 39: 848-853.

[37] El Qada E. N., Allen S. J., Walker G. M., (2006), Adsorption of Methylene Blue onto activated carbon produced from steam activated bituminous coal: A study of equilibrium adsorption Isotherm. *Chem. Eng. J*.124: 103-110.

[38] Gupta V. K., Jain C. K., Ali I., Chandra S., Agarwal S., (2002), Removal of Lindane and Malathion from wastewater using bagasse fly ash-a sugar industry waste. *Water Res*. 36: 2483-2490.

[39] Hameed B. H., (2009), Evaluation of papaya seed as a non conventional low cost adsorbent for removal of MB, *J. Hazard. Mater*. 162: 939-944.

[40] Bagha A. R. T., Nikkar H., Mahmoodi N. M., Markazi M., Menger F. M., (2011), The sorption of cationic dyes onto kaolin: Kinetic, isotherm and thermodynamic studies. *Desalination* 266: 274-280.

[41] Hema M., Arivoli S., (2007), Comparative study on the adsorption kinetics and thermodynamics of dyes onto acid activated low cost carbon. *Int. J. Phys. Sci*. 2: 10-17.

[42] Abasi C. Y., Abia A. A., Igwe J. C., (2011), Adsorption of Iron (III), Lead (II) and Cadmium (II) Ions by Unmodified Raphia Palm (Raphia hookeri) Fruit Endocarp. *Environ. Res. J*. 5: 104-113.

[43] Al Othman Z. A., Hashem A., Habila M. A., (2011), Kinetic, Equilibrium and Thermodynamic Studies of Cadmium (II) Adsorption by Modified Agricultural Wastes. *Molecules*. 16: 10443-10456

[44] Offurum J. C., Iheme C., Chikaire A. J., (2011), Iotherm and thermodynamics studies for adsorption of solid particles on cow bone granule. *Contin. J. Eng. Sci*. 6: 31-36.

[45] Chen A. H., Chen S. M., (2009), Biosorption of azo dyes from aqueous solution by glutaraldehyde-crosslinked chitosans. *J. Haz. Mater*. 172: 1111-1121.

Cite this article as: Gh. Kiani: Adsorption kinetics and thermodynamics of Malachite Green from aqueous solutions onto expanded graphite nanosheets.
Int. J.Nano Dimens. 6(1): 55-66, Winter 2015